

# Phase diagram of bosonic matter with additional derivative interaction

L. M. Satarov,<sup>1</sup> I. N. Mishustin,<sup>1</sup> and H. Stoecker<sup>1</sup>

<sup>1</sup>*Frankfurt Institute for Advanced Studies,  
D-60438 Frankfurt am Main, Germany*

Equation of state of uncharged bosonic matter (BM) is studied within a field-theoretical approach in the mean-field approximation. Interaction of bosons is described by a scalar field  $\sigma$  with a Skyrme-like potential which contains both attractive and repulsive terms. Additionally we introduce the derivative interaction (DI) by including factor  $(1 + \lambda\sigma)^{-1}$  in the kinetic part of Lagrangian where  $\lambda > 0$  is the model parameter. Numerical calculations are made for strongly interacting matter composed of  $\alpha$  particles. It is shown that ground-state binding energy and equilibrium density of such matter drop with increasing  $\lambda$ . The liquid-gas phase transition (LGPT) and the Bose-Einstein condensation (BEC) are studied by using different thermodynamic variables. We calculate also spinodal lines which give boundaries of metastable states. It is demonstrated that critical temperature decreases with  $\lambda$ . Both LGPT and bound condensate states disappear above certain maximum value of  $\lambda$ .

## I. INTRODUCTION

The derivative (momentum-dependent) interactions are widely used in modern nuclear and particle physics. They are introduced e.g. for implementing the effects of binary scatterings with nonzero angular momenta ( $p, d...$  waves), for accounting finite sizes of hadrons, for analyzing surface properties of nuclei etc. One example of such interaction is the pion-nucleus optical potential of the Kislinger type [1]. Inclusion of additional gradient terms of the potential lead to better agreement with observed data on  $\pi A$  elastic scattering. The phenomenological Skyrme potentials of NN interactions [2, 3] also contain momentum-dependent terms. In addition, one should mention the relativistic mean-field models [4, 5] with derivative couplings of fermion and meson fields. By using such interactions one can

achieve reasonable values of the nuclear matter compressibility, overestimated in standard Walecka calculations.

A large variety of models with DI have been formulated in cosmology. For example, the 'kinetic K-essence' models [6, 7] with noncanonical kinetic energies of scalar fields were introduced to explain the Universe acceleration, observed in red-shift measurements of distant supernovae. The authors of Ref. [8] introduce the coupling between the cosmic curvature and the density of the scalar field  $\sigma$ . This leads to the kinetic part of matter Lagrangian with an additional factor  $F = (1 + A\sigma)^{-1}$ . Below we use this result to investigate BEC and phase transition of bosonic matter with DI.

In Refs. [9, 10] we developed the mean-field models to describe properties of homogeneous matter composed of  $\alpha$  particles. We use the standard standard kinetic energy and describe interactions of particles by using the Skyrme potential which is attractive at small densities. Similarly to atomic  ${}^4\text{He}$ , such matter undergoes both the LGPT and the BEC transition. In Refs. [11, 12] we have studied the  $\alpha$ -nucleon matter. It is shown that at large enough attraction between  $\alpha$  particles and nucleons the nuclear ground state contains the admixture of  $\alpha$ 's. A similar effect has been predicted within the nuclear lattice model in Ref. [13].

In our recent publication [14] we studied characteristics of ' $\alpha$ -conjugate' nuclei (with even proton and neutron numbers  $Z = N = A/2$ ). It is believed that such nuclei may contain Bose-condensed clusters of  $\alpha$  particles (see Ref. [15] and references therein). We have considered ground states of these nuclei as Q-balls<sup>1</sup> (or Q-shells) made of charged  $\alpha$  particles. It was shown that typically such Q-balls have bindings which noticeable overestimate the observed binding energies of  $\alpha$ -conjugate' nuclei. In addition, the standard calculation predicts too small surface tension which leads to unrealistically narrow widths<sup>2</sup> of Q-ball surfaces. This unsatisfactory result has been corrected in Ref. [14] by introducing an artificially enhanced gradient term of the energy density. We believe that future covariant calculations with derivative interaction may resolve this problem.

In the present article we study the sensitivity of the phase diagram of bosonic matter to DI. As far as we know, this has not been done up to now by other authors. We consider the particular case of matter composed of  $\alpha$  particles and use the parameters of their potential from our previous publications [10, 14].

---

<sup>1</sup> The 'Q-balls' have been introduced in Refs. [16–18] as soliton-like bound states of scalar bosons. Currently they are considered as promising candidates for stable dark matter.

<sup>2</sup> less than the size of the  $\alpha$  particle

The paper is organized as follows. In Sec. II A we derive the generalized Klein-Gordon equation for the bosonic field. It is obtained using the kinetic term of the Lagrangian with the derivative factor. In the next section we consider the thermodynamic functions for cold BM. In Sec. II C we calculate numerically properties of BM at zero temperature for different sets of model parameters. In Sec. III we extend our formalism to nonzero temperatures. The resulting formulae are applied in Sec. IV for investigating the phase diagram of warm BM.

## II. COLD BOSONIC MATTER IN THE MEAN-FIELD APPROXIMATION

### A. Equations of motion for scalar field

In this paper we consider a system of uncharged bosonic particles with strong self-interaction. We apply a field-theoretical approach denoting by  $\phi(x)$  the scalar field at the space-time point  $x^\nu = (t, \mathbf{r})^\nu$ . The Lagrangian density of the system is assumed to be of the generic form ( $\hbar = c = 1$ ):

$$\mathcal{L} = \frac{1}{2}F(\sigma)\chi - U(\sigma), \quad (1)$$

where  $\sigma = \phi\phi^*$ ,  $\chi = \partial_\nu\phi\partial^\nu\phi^*$  and  $U(\sigma)$  is the mean-field potential, which contains the mass term and self-interaction terms. One can regard the quantity  $[F(\sigma) - 1]\chi/2$  as an additional DI proportional to particle four-momentum squared. In the majority of theoretical models it is implicitly assumed that  $F = 1$  i.e. one neglects any modification of the kinetic part of Lagrangian as compared to its canonical form  $\mathcal{L}_{\text{kin}} = \chi/2$ .

By using Eq. (1) one can write the expressions for the four current  $J^\nu$  and the energy-momentum tensor  $T^{\mu\nu}$ :

$$J^\nu = \frac{iF}{2}(\phi\partial^\nu\phi^* - \phi^*\partial^\nu\phi), \quad T^{\mu\nu} = \frac{F}{2}(\partial^\mu\phi\partial^\nu\phi^* + \partial^\mu\phi^*\partial^\nu\phi) - g^{\mu\nu}\mathcal{L}. \quad (2)$$

The Euler-Lagrange equation leads to the equation of motion for scalar fields. One gets the generalized Klein-Gordon equation (KGE)

$$\partial_\nu(F\partial^\nu\phi) + (2U' - F'\chi)\phi = 0, \quad (3)$$

where primes denote derivatives with respect to  $\sigma$ .

The stationary solution of the KGE is obtained by the substitution [18]

$$\phi = e^{i\mu t}\varphi(\mathbf{r}), \quad (4)$$

where  $\varphi = \sqrt{\sigma}$  is a real function of spatial coordinates  $\mathbf{r}$ . The constant  $\mu$  is in fact the chemical potential characterizing the bound state of the Bose-Einstein condensate at zero temperature (see below). Substituting (4) into Eq. (3) one gets the stationary KGE for  $\varphi$ <sup>3</sup>

$$\nabla(F\nabla\varphi) + [\mu^2(F\sigma)' - 2U' - F'(\nabla\varphi)^2]\varphi = 0. \quad (5)$$

Using (4) in Eqs. (2) gives the expressions for the number density  $n$  and the energy density  $\varepsilon$  of bosonic particles

$$n = J^0 = \mu F\sigma, \quad (6)$$

$$\varepsilon = T^{00} = \frac{\mu n}{2} + U + \frac{F}{2}(\nabla\varphi)^2. \quad (7)$$

It is interesting that Eq. (5) can be also obtained by minimizing the functional of thermodynamic potential  $\Omega = \varepsilon - \mu n$  with respect to arbitrary variation  $\delta\phi$  at constant  $\mu$ . One gets the relation

$$\int dV \delta\Omega = \int dV \delta \left[ \frac{F}{2}(\nabla\varphi)^2 - p(\mu, \sigma) \right] = 0. \quad (8)$$

where

$$p(\mu, \sigma) = \frac{\mu^2 F\sigma}{2} - U(\sigma). \quad (9)$$

Let us consider now the homogeneous BM at zero temperature. In this case, substituting  $\nabla\varphi = 0$ , we get the 'gap' equation determining the equilibrium condensate density  $\sigma = \sigma(\mu)$  and pressure  $p$  at given  $\mu$

$$\left( \frac{\partial p}{\partial \sigma} \right)_\mu = \frac{\mu^2(F\sigma)'}{2} - U'(\sigma) = 0. \quad (10)$$

Using Eqs. (6), (9)–(10) one can prove the condition of thermodynamic consistency  $dp = n d\mu$ .

It is convenient to rewrite Eq. (10) in the form

$$\mu = M(\sigma), \quad M(\sigma) = \sqrt{\frac{2U'(\sigma)}{(F\sigma)'}}. \quad (11)$$

As we will see below  $M(\sigma)$  plays a role of the effective mass of bosonic quasiparticles. The first relation in (11) may be considered as condition of BEC.

---

<sup>3</sup> In case  $F = 1$  one obtains the equation for the Q-ball profile from Ref. [18].

## B. Thermodynamic functions and ground states at $T = 0$

At thermal equilibrium all particles in cold BM are in the Bose-condensed state with zero momentum (within the mean-field approximation). We introduce the following parametrization of functions  $F^4$  and  $U$ :

$$F(\sigma) = (1 + \lambda\sigma)^{-1}, \quad U(\sigma) = \frac{\sigma}{2} \left( m^2 - \frac{a\sigma}{2} + \frac{b\sigma^\alpha}{\alpha + 1} \right), \quad (12)$$

where  $m$  is the vacuum mass of bosons and  $a, b, \lambda$  and  $\alpha$  are positive model parameters (we consider only the values  $\alpha > 1$ ). Note that the second and third terms of Skyrme potential  $U(\sigma)$  describe respectively the attractive and repulsive interactions of particle. The limit  $\lambda = 0$  corresponds to the case without DI. It was considered in our previous publications on pionic [19] and  $\alpha$ -particle [9, 10, 14] systems<sup>5</sup>. Below we show that the presence of the suppression factor  $F$  leads effectively to an additional repulsion.

Using formulae of preceding section, one gets the equations

$$\mu = M(\sigma) = (1 + \lambda\sigma)\sqrt{m^2 - a\sigma + b\sigma^\alpha}, \quad (13)$$

determining the scalar density  $\sigma$  and the effective mass  $M$  as functions of the chemical potential  $\mu^6$ . According to Eq. (13) characteristics of the Bose condensate are sensitive to  $\lambda$ . One can see that at fixed  $\sigma$  increasing  $\lambda$  leads to increase of the effective mass and therefore, to reducing binding energy  $m - M$ . As a consequence, the LGPT lines, appearing in the present model, move with growing  $\lambda$  to the region of larger chemical potentials (see below Figs. 6–8).

Finally, we get the following equations for density  $n$ , pressure  $p$  and energy density  $\varepsilon$ :

$$n = \sigma\sqrt{m^2 - a\sigma + b\sigma^\alpha}, \quad (14)$$

$$p = \frac{Mn}{2} - U, \quad \varepsilon = \frac{Mn}{2} + U. \quad (15)$$

Let us consider properties of the ground state (GS) of cold BM, i.e. the state of minimum energy per particle or zero pressure. Using the above equations one can determine the

<sup>4</sup> It is interesting that the same parametrization of the derivative factor has been used in the cosmological model of Ref. [8].

<sup>5</sup> Note that only the case  $\alpha = 2$  has been considered in Refs. [10, 14, 19].

<sup>6</sup> In general, Eq. (13) has several solutions for  $\sigma = \sigma(\mu)$ . In real calculations we use  $\sigma$  as input variable and determine  $\mu$  as function of  $\sigma$ .

ground-state scalar density  $\sigma_0$  and the corresponding chemical potential  $\mu_0$  by solving the system of equations

$$\mu_0 = (1 + \lambda\sigma_0)\sqrt{2U'_0}, \quad p_0 = \frac{\mu_0^2\sigma_0}{2(1 + \lambda\sigma_0)} - U_0 = 0, \quad (16)$$

where quantities with index zero are taken at  $\sigma = \sigma_0$ . Eliminating the chemical potential gives the relation

$$1 + \lambda\sigma_0 = \frac{U_0}{\sigma_0 U'_0}, \quad (17)$$

which determines the dependence of  $\sigma_0$  on the parameter  $\lambda$ . Using further the explicit form of  $U(\sigma_0)$  from Eq. (12) we get the expression

$$\lambda(m^2 - a\sigma_0 + b\sigma_0^\alpha) = \frac{a}{2} - \frac{\alpha b\sigma_0^{\alpha-1}}{\alpha + 1}, \quad (18)$$

which was solved numerically at fixed parameters  $a, b, \lambda$ .

In the limit  $\lambda \rightarrow 0$  characteristics of GS can be found analytically for any  $\alpha$ . Below we mark the corresponding values by tilde. Substituting  $\lambda = 0$  in Eqs. (16), (18) leads to the relation

$$\tilde{\sigma}_0 = \left[ \frac{(1 + \alpha)a}{2\alpha b} \right]^{\frac{1}{\alpha - 1}}. \quad (19)$$

In the present paper we chose  $a, b$  by fixing characteristics of the GS at zero derivative strength  $\lambda$ . Namely, we assume the same binding energy per particle  $W_0 = m - \tilde{\mu}_0$  and density  $n_0$  for all  $\alpha$ . One can write down the explicit relations

$$a = \frac{2\alpha}{\alpha - 1} \frac{(m^2 - \tilde{\mu}_0^2)}{\tilde{\sigma}_0}, \quad (20)$$

$$b = \frac{\alpha + 1}{\alpha - 1} \frac{(m^2 - \tilde{\mu}_0^2)}{\tilde{\sigma}_0^\alpha}, \quad (21)$$

where  $\tilde{\sigma}_0 = n_0/\tilde{\mu}_0$ .

As an example, we use the GS characteristics determined in variational calculations of cold  $\alpha$  matter in Ref. [20]<sup>7</sup>:

$$W_0 = 19.7 \text{ MeV}, \quad n_0 = 0.036 \text{ fm}^{-3}. \quad (22)$$

Using this procedure and substituting the particle mass  $m = m_\alpha = 3.7273 \text{ GeV}$  we get numerical values of  $a, b$  for two parameter sets with  $\alpha = 1.1$  and  $\alpha = 2$  (see Table I). Note that

---

<sup>7</sup> These calculations were based on phenomenological pair potentials adjusted to  $\alpha\alpha$  phase shifts observed at low energies.

both these sets correspond to the same value of scalar density

$$\tilde{\sigma}_0 \simeq 9.658 \cdot 10^{-3} \text{ GeV}^{-1} \text{ fm}^{-3}. \quad (23)$$

The case of nonzero  $\lambda$  can be discussed qualitatively in the nonrelativistic approximation (NRA). It has a good accuracy, at least for  $\alpha$  matter at not too large scalar densities. Within the NRA  $|\mu_0 - m| \ll m$ , and one can omit the terms containing  $\sigma_0$  in the left hand side of Eq. (18). This leads to the approximate formulae

$$\sigma_0 \simeq \tilde{\sigma}_0 \left(1 - \frac{\lambda}{\lambda_m}\right)^{\frac{1}{\alpha-1}}, \quad (24)$$

where  $\tilde{\sigma}_0$  is defined in (19) and  $\lambda_m = a/(2m^2)$  is the maximal possible value of  $\lambda$  at which bound states of BM exist ( $\mu_0 < m$ ). One can see that  $\sigma_0$  monotonically drops with  $\lambda$ . The last column of Table I gives values of  $\lambda_m$  for two choices of  $\alpha$  considered in this paper. One can see that harder Skyrme potentials (with larger  $\alpha$ ) lead to reduced values of  $\lambda_m$ <sup>8</sup>.

TABLE I. Parameters of Skyrme potential and maximal value of derivative strength  $\lambda_m$ .

$\alpha$	$a$ (GeV <sup>3</sup> fm <sup>3</sup> )	$b$ (GeV <sup><math>\alpha+2</math></sup> fm <sup>3<math>\alpha</math></sup> )	$\lambda_m$ (GeVfm <sup>3</sup> )
1.1	331.9	503.5	11.9
2	60.34	4661	2.16

Within the considered model one can easily calculate the sound velocity  $c_s$ . At  $T = 0$  one may use the expressions [22]

$$c_s^2 = \frac{dp}{d\varepsilon} = \frac{nd\mu}{\mu dn}. \quad (25)$$

Substituting  $\mu = M(\sigma)$ ,  $n = MF\sigma$  and using the relation  $(F\sigma)' = F^2$  we obtain the equation

$$c_s^2 = \left[1 + \frac{MF}{M'\sigma}\right]^{-1}. \quad (26)$$

One can see that unstable spinodal states with  $c_s^2 < 0$  occur at  $1 + MF/M'\sigma < 0$ . Within the NRA one obtains

$$c_s^2 \simeq \frac{M'(\sigma)\sigma}{mF(\sigma)}. \quad (27)$$

<sup>8</sup> Using the data of Table I one can show that the factor  $F$  deviates only slightly from unity at  $\sigma \lesssim \sigma_0$ .

Nevertheless, the derivative corrections have a relatively large effect even in NRA. This follows from the fact that zero-order terms in  $\lambda$  (originating from large mass term of Skyrme potential) effectively cancel out in pressure and binding energy (see Eqs. (16)–(18)).

### C. Numerical results

In this section we present results of numerical calculations for cold BM obtained within the scheme described in preceding section. We apply the model parameters given in Table I. Table II shows the characteristics of GS calculated for different  $\alpha$  and  $\lambda$ . One can see that the ground-state binding energy, density and sound velocity of BM are rather sensitive to the derivative strength  $\lambda$ . According to our calculations, all these quantities drop with increasing  $\lambda$ .

TABLE II. Ground-state characteristics of BM at  $T = 0$ .

$\lambda$ (GeVfm <sup>3</sup> )	$\alpha = 1.1$			$\alpha = 2$		
	$\mu_0 - m$ (MeV)	$n_0 \times 10^2$ (fm <sup>-3</sup> )	$c_s \times 10^2$	$\mu_0 - m$ (MeV)	$n_0 \times 10^2$ (fm <sup>-3</sup> )	$c_s \times 10^2$
0	-19.70	3.60	7.63	-19.70	3.60	10.3
0.5	-12.35	2.36	6.07	-11.73	2.78	7.96
1	-7.58	1.96	4.76	-5.81	1.52	5.63

A more detailed information is given in Figs. 1–4. In particular, Fig. 1 show isotherms  $T = 0$  on the  $(\mu, \sigma)$  plane for different parameters  $\alpha$  and  $\lambda$ . At  $\lambda = 0$  the positions of GS coincide for  $\alpha = 1.1$  and  $\alpha = 2$ . This follows from the procedure of choosing parameters of the Skyrme potential used in present paper. One can see that each line in Fig. 1 has upper and low parts. The low parts with  $\sigma'(\mu) < 0$  correspond to unstable (spinodal) states with  $c_s^2 < 0$ . Within the present model, at  $T = 0$  the GS is simultaneously the binodal point of the LGPT. Note that pressure of BM changes sign at GS points. The states with  $\mu < \mu_0$  on the upper branch of  $\sigma(\mu)$  are in fact metastable<sup>9</sup>.

The same conclusions can be made from Fig. 2 which shows the sound velocity squared, calculated by using Eq. (26). The unstable spinodal states correspond to points below the horizontal line  $c_s^2 = 0$ . One can see that sound velocity vanishes at the boundary between metastable and spinodal states. At this boundary the chemical potential takes its minimal possible value.

The conclusion that GS is the binodal point of the LGPT can also be made from Figs. 3–4 which show the isotherms of pressure on the  $(\mu, p)$  and  $(n, p)$  planes. The binodal states of

<sup>9</sup> The metastable states with negative pressure have been observed in liquid <sup>4</sup>He [21].

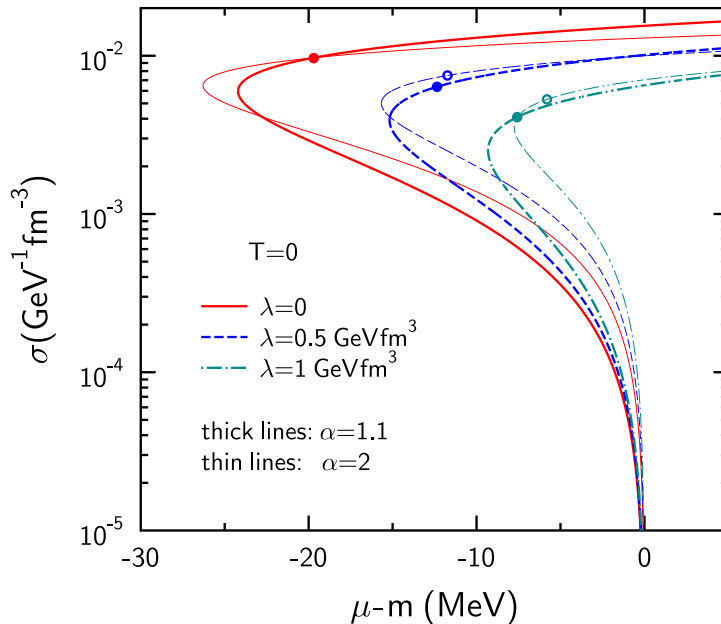


FIG. 1. The scalar density of cold BM as the function of chemical potential  $\mu$  for different values of derivative strength  $\lambda$ . Bold and thin lines are calculated from Eq. (13) with  $\alpha = 1.1$  and  $\alpha = 2$ , respectively. Dots show positions of GS on the  $(\mu, \sigma)$  plane.

LGPT originate from intersecting pressure lines with small and large slopes in Fig. 3. This is a graphic representation of the Gibbs construction rule for phase equilibrium between the liquid and gas phases (see Sec. IV). At  $T = 0$  both phases have vanishing pressure. The spinodal 'states' correspond to points between two kinks of pressure slopes in the  $(\mu, p)$  plane. For all considered values of  $\lambda$  and  $\alpha$  one gets the 'gas-like' spinodal boundary at the same point with  $\mu = m$  and  $p = 0$ .

### III. THERMODYNAMIC FUNCTIONS AT NONZERO TEMPERATURES

Below we modify the formalism, suggested in Ref. [10] to describe warm  $\alpha$  matter without DI. At temperatures  $T \neq 0$ , in addition to spatially homogeneous BEC state  $\phi_c$  with vanishing momentum, it is necessary to take into account thermal fluctuations of scalar fields. We use a plane-wave decomposition of  $\phi$  in terms of creation ( $a_{\mathbf{k}}^+$ ) and annihila-

tion ( $a_{\mathbf{k}}$ ) operators [23]

$$\phi(x) = \phi_c(t) + \sum_{\mathbf{k}} \frac{1}{\sqrt{2F E_{\mathbf{k}}}} (a_{\mathbf{k}} e^{-i\mathbf{k}x} + a_{\mathbf{k}}^{\dagger} e^{i\mathbf{k}x}), \quad (28)$$

where  $\phi_c = \exp(i\mu t)\sqrt{\sigma_c}$  is proportional to the square root of condensate scalar density  $\sigma_c$ ,  $k^0 = E_{\mathbf{k}} \equiv \sqrt{M^2 + \mathbf{k}^2}$  ( $M = M(\sigma)$  is the effective mass of bosons defined in Eq. (13)). For brevity we introduce the notation

$$\sum_{\mathbf{k}} = \frac{g}{(2\pi)^3} \int d^3k, \quad (29)$$

where  $g$  is the spin-isospin statistical weight of a boson particle ( $g = 1$  for alphas). As compared to Ref. [10], an additional factor  $F$  is inserted into the denominator of Eq. (28)<sup>10</sup>.

In the following we denote by angular brackets the statistical averaging in the grand-canonical ensemble. Within the mean-field approximation one gets the following expression for the particle momentum distribution at given chemical potential  $\mu$  and temperature  $T$ :

$$n_{\mathbf{k}} = \langle a_{\mathbf{k}}^{\dagger} a_{\mathbf{k}} \rangle = \left[ \exp\left(\frac{E_{\mathbf{k}} - \mu}{T}\right) - 1 \right]^{-1}. \quad (30)$$

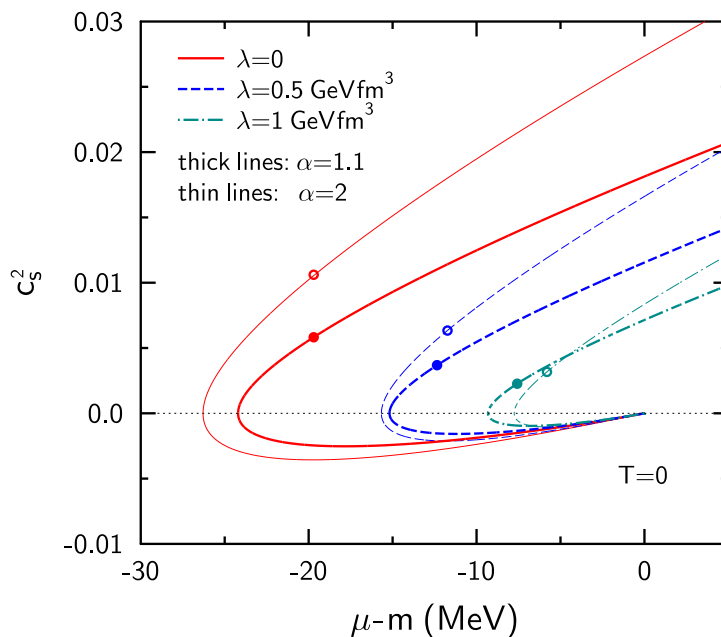


FIG. 2. Same as Fig. 1, but for the sound velocity squared as the function of chemical potential.

<sup>10</sup> This factor is introduced to preserve the standard equal-time commutation relation [24]  $[\Pi(x), \phi(x')] = i\delta(\mathbf{r} - \mathbf{r}')$ , where  $\Pi(x) = \frac{\delta\mathcal{L}}{\delta\dot{\phi}^*(x)} = F\dot{\phi}/2$  is the canonical momentum conjugated to  $\phi$ .

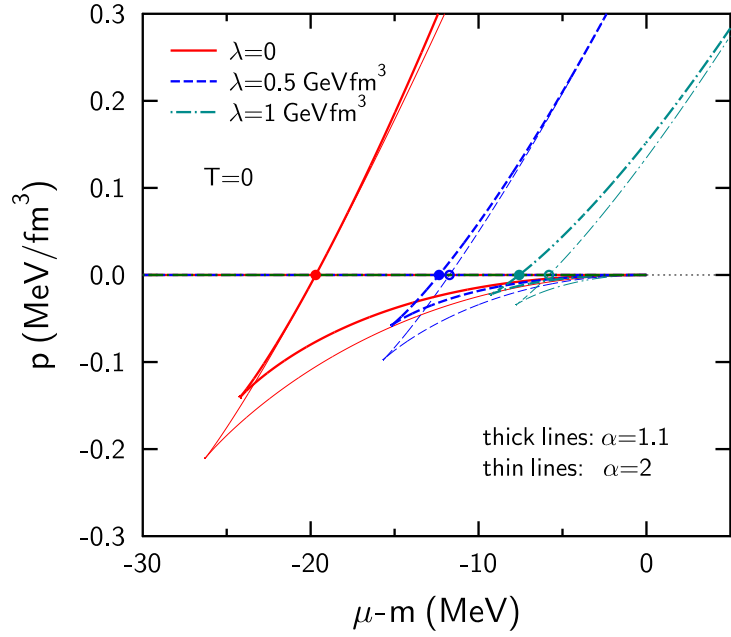


FIG. 3. Pressure of cold BM as the function of chemical potential at different values of parameter  $\lambda$ . Thick and thin lines are calculated with  $\alpha = 1.1$  and  $\alpha = 2$ , respectively. Full dots show positions of GS.

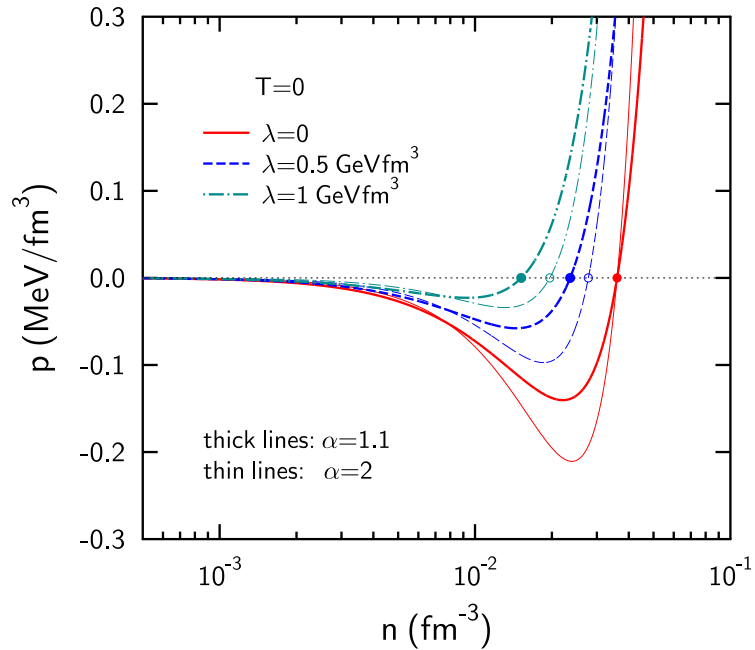


FIG. 4. Same as Fig. 3, but for pressure as the function of density.

This distribution depends on the scalar density  $\sigma = \langle \phi^2 \rangle$  via the mass  $M(\sigma)$  entering  $E_{\mathbf{k}}$ .

Note that allowed states of BM should satisfy the condition  $\mu \leq M(\sigma)$  where the equal sign corresponds to states with BEC. We shall see that this takes place at high enough  $\mu$  or at temperatures below the condensation temperature  $T_{\text{BEC}}(\mu)$ .

Using Eqs. (28), (30) one obtains the relation:

$$\sigma = \sigma_c + \sigma_{\text{th}}, \quad (31)$$

where

$$\sigma_{\text{th}}[T, \mu, M(\sigma)] = \sum_{\mathbf{k}} \frac{n_{\mathbf{k}}}{FE_{\mathbf{k}}} = \frac{g}{2\pi^2 F} \int_M^{\infty} \frac{dE \sqrt{E^2 - M^2}}{\exp\left(\frac{E - \mu}{T}\right) - 1}. \quad (32)$$

The first condensate term in the right hand side of (31) vanishes for  $T > T_{\text{BEC}}$ . In this case one obtains the self-consistent gap equation  $\sigma = \sigma_{\text{th}}$  for  $\sigma(T, \mu)$ . At  $T < T_{\text{BEC}}$  the scalar density is determined directly from the condition  $M(\sigma) = \mu$ . Then Eq. (31) may be regarded as the equation for determining  $\sigma_c(T, \mu)$ .

In the case  $T \ll M$  one can use NRA by taking lower-order terms in  $T/M$  in calculating thermodynamic integrals. This leads to the approximate relation

$$\sigma_{\text{th}} \simeq \frac{g}{FM\lambda_T^3} g_{3/2}(z), \quad (33)$$

where  $z \leq 1$  is the nonrelativistic fugacity and  $\lambda_T = \lambda_T(T, M)$  is the thermal wave length:

$$z = \exp\left(\frac{\mu - M}{T}\right), \quad \lambda_T = \sqrt{\frac{2\pi}{MT}}. \quad (34)$$

The dimensionless function (polylogarithm)  $g_{\beta}(z)$  is defined as

$$g_{\beta}(z) \equiv \frac{1}{\Gamma(\beta)} \int_0^{\infty} dx \frac{x^{\beta-1}}{z^{-1}e^x - 1} = \sum_{k=1}^{\infty} z^k k^{-\beta}. \quad (35)$$

At low fugacities  $g_{\beta}(z) \simeq z$  is small, in the degenerate limit  $z \rightarrow 1$  one has  $g_{\beta}(z) \simeq \xi(\beta)$  where  $\xi(\beta)$  is the Riemann function.

By substituting (28) into the first equality of (2) for  $\nu = 0$  and performing the grand-canonical averaging one gets the relation for the particle number density:

$$n = n_c + n_{\text{th}}, \quad (36)$$

where  $n_c = \mu F \sigma_c$  is the Bose-condensed part of density and

$$n_{\text{th}}(T, \mu, M) = \sum_{\mathbf{k}} n_{\mathbf{k}} = \frac{g}{2\pi^2} \int_M^{\infty} \frac{dE E \sqrt{E^2 - M^2}}{\exp\left(\frac{E - \mu}{T}\right) - 1}. \quad (37)$$

Within the NRA one gets the approximate expression  $n_{\text{th}} \simeq \frac{g}{\lambda_T^3} g_{3/2}(z)$ . For states with  $n\lambda_T^3 \gtrsim 1$ , the effects of quantum statistics are important.

One gets explicit expression for the BEC boundary by substituting  $n_c = 0, M = \mu$  in Eqs. (36)–(37). One gets the following formula for the threshold temperature of BEC in NRA [10]

$$T_{\text{BEC}} \approx \frac{2\pi}{\mu} \left( \frac{n}{g\xi(3/2)} \right)^{2/3}. \quad (38)$$

The pressure  $p$  is determined by spatial components of the energy-momentum tensor  $T_{\alpha\alpha}$  which in turn can be calculated from the Lagrangian. One has in the mean-field approximation

$$p = \frac{1}{3} \langle T_{xx} + T_{yy} + T_{zz} \rangle = p_{\text{ex}}(\sigma) + p_{\text{th}}(T, \mu, M). \quad (39)$$

Here the first term is the so-called excess pressure

$$p_{\text{ex}}(\sigma) = \frac{M(\sigma)^2 F \sigma}{2} - U(\sigma). \quad (40)$$

It is equal to the pressure of cold homogeneous BM with scalar density  $\sigma$  (see Eqs. (14) and (15))<sup>11</sup>. The second, thermal part takes the form

$$p_{\text{th}}(T, \mu, M) = \frac{F}{6} \langle \nabla\phi \nabla\phi^* \rangle = \sum_{\mathbf{k}} \frac{\mathbf{k}^2}{3E_{\mathbf{k}}} n_{\mathbf{k}} = \frac{g}{6\pi^2} \int_M^\infty \frac{dE (E^2 - M^2)^{3/2}}{\exp\left(\frac{E - \mu}{T}\right) - 1}. \quad (41)$$

In the second equality we applied the equation (28). The calculation shows that the excess pressure dominates at small temperatures. One can see that expressions for  $n_{\text{th}}$  and  $p_{\text{th}}$  coincide with the corresponding ideal gas expressions after the replacement  $m \rightarrow M$  (note that factors  $F$  cancel out in Eqs. (37) and (41)). Within the NRA one obtains the approximate relation  $p_{\text{th}} \simeq \frac{gT}{\lambda_T^3} g_{5/2}(z)$ . In the Boltzmann limit (at  $n\lambda_T^3 \ll 1$ ) one has  $p_{\text{th}} \simeq n_{\text{th}}T$ . One can check the validity of the relation  $(\partial p_{\text{th}}/\partial M)_{T, \mu} = -MF\sigma_{\text{th}}$ . It guarantees the thermodynamic consistency,  $(\partial p/\partial \mu)_T = n$ , of the present model [10].

#### IV. PHASE DIAGRAM OF BOSONIC MATTER

Below we present the results of numerical calculations based on the formulae of previous section. As in Sec. IIC, we compare the calculations for two choices of the Skyrme potential

<sup>11</sup> This term vanishes for non-interacting BM with  $a, b, \lambda \rightarrow 0$ . Note that Bose-condensed particles with zero momentum contribute the pressure only indirectly, via the scalar density component  $\sigma_c$ .

parameter  $\alpha = 1.1$  and  $\alpha = 2$ . Figure 5 shows the BEC lines at various  $\lambda$  and  $\alpha$ . Note that lower (decreasing) parts of these lines are unstable.

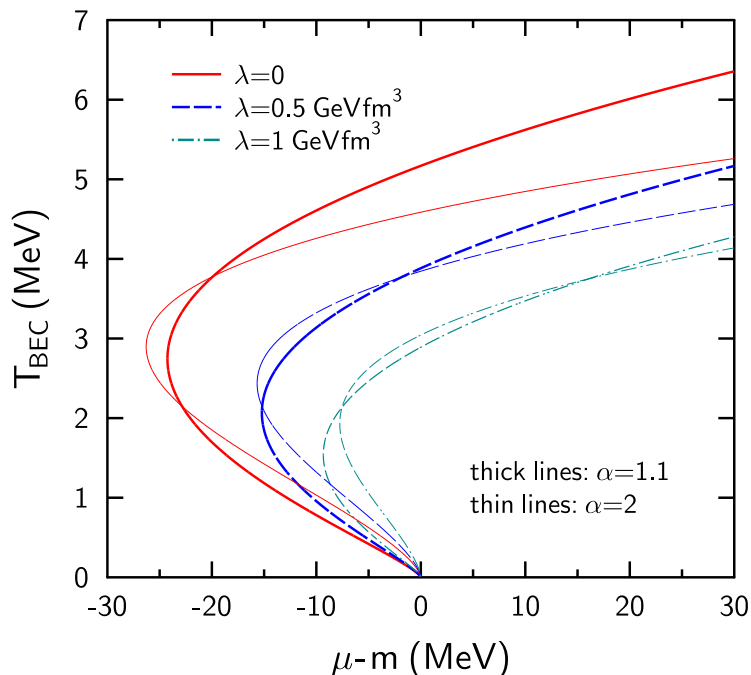


FIG. 5. The BEC transition temperatures as functions of  $\mu$ . Thick and thin lines correspond to  $\alpha = 1.1$  and  $\alpha = 2$  respectively.

To demonstrate the procedure of calculating phase diagrams we consider in Fig. 6 the particular case of the isotherm  $T = 5$  MeV for  $\alpha = 2$  and two values of  $\lambda$ . The vertical lines in the  $(\mu, \sigma)$  plane correspond to equilibrium mixed-phase states of the LGPT. The upper and lower ends of these lines represent the liquid-like (L) and gas-like (G) binodal states of LGPT. The corresponding scalar densities  $\sigma_i$  ( $i = L, G$ ) are found from the Gibbs condition of the phase equilibrium

$$p [T, \mu, \sigma_L(T, \mu)] = p [T, \mu, \sigma_G(T, \mu)] \quad . \quad (42)$$

Numerically we solve this equation by finding intersection of two branches of isotherms with different slopes in the  $(\mu, p)$  plane. In this way we determine the binodal line of LGPT as well as the spinodal boundaries of LGPT. One can indeed see from Fig. 6 that the position of the LGPT shifts to smaller  $|\mu - m|$  with raising  $\lambda$ .

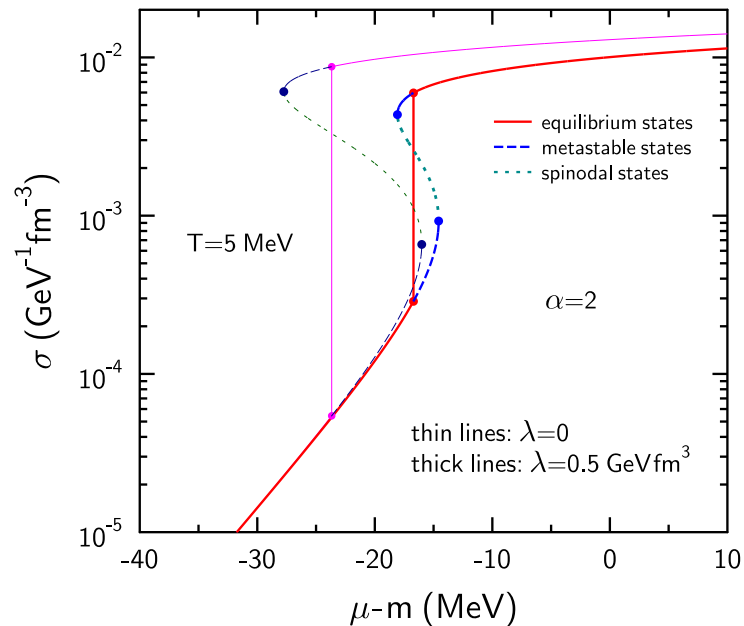


FIG. 6. The isotherms  $T = 5$  MeV on the  $(\mu, \sigma)$  plane for  $\alpha = 2$ . The vertical lines correspond to equilibrium mixed-phase states of LGPT. The dashed and dotted curves represent the metastable and spinodal (unstable) states, respectively.

The critical point (CP) of the LGPT is the state with maximum temperature where the solution of Eq. (42) still exists. The binodal scalar densities coincide in this case:

$$\sigma_L(T_c, \mu_c) = \sigma_G(T_c, \mu_c). \quad (43)$$

The present model leads to characteristics of CP listed in Tables III and IV.

TABLE III. Characteristics of the critical points of LGPT for  $\alpha = 1.1$ .

$\lambda$ ( $\text{GeVfm}^3$ )	$T_c$ (MeV)	$\mu_c - m$ (MeV)	$n_c \times 10^2$ ( $\text{fm}^{-3}$ )	$p_c \times 10^2$ ( $\text{MeVfm}^{-3}$ )
0	9.90	-37.3	0.90	2.36
0.5	6.30	-22.1	0.60	1.00
1	3.95	-12.8	0.39	0.41

The phase diagrams of BM in the  $(\mu, T)$  plane predicted by our calculation are shown in Figs. 7 and 8 for  $\alpha = 1.1$  and  $\alpha = 2$ , respectively. In addition we show the BEC lines and boundaries of metastable regions. The phase transition lines starts at zero-temperature

TABLE IV. Characteristics of the critical points of LGPT for  $\alpha = 2$ .

$\lambda$ ( $\text{GeV fm}^3$ )	$T_c$ (MeV)	$\mu_c - m$ (MeV)	$n_c \times 10^2$ ( $\text{fm}^{-3}$ )	$p_c \times 10^2$ ( $\text{MeV fm}^{-3}$ )
0	13.79	-49.0	1.24	5.73
0.5	8.46	-25.9	0.97	2.75
1	4.49	-10.7	0.71	1.06

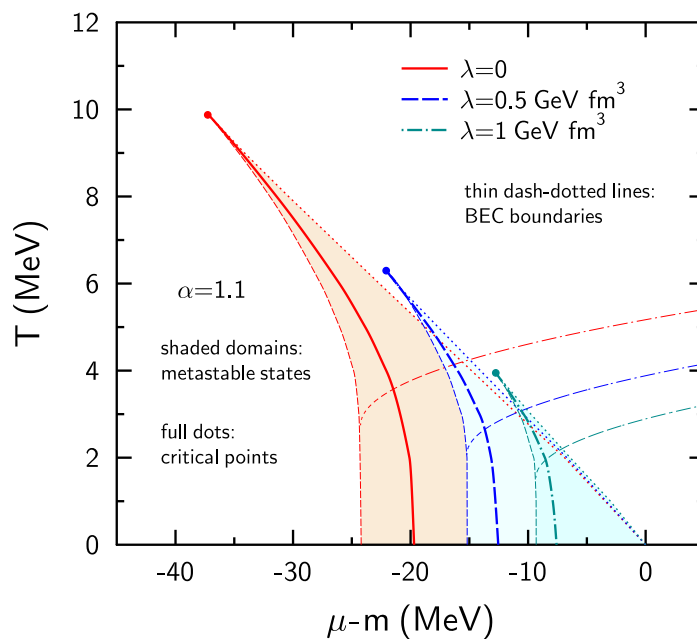


FIG. 7. Phase diagrams of bosonic matter on the  $(\mu, T)$  plane for  $\alpha = 1.1$  and different values of the derivative strength  $\lambda$ . Thick lines correspond to mixed-phase states of the LGPT. Shading show regions of metastable states. Dots represent positions of critical points. The dash-dotted lines show boundaries of BEC states.

GS points. The gas-like spinodals for different  $\lambda$  ends at the vacuum point  $\mu = m, T = 0$ . One can see that shifts of phase diagrams to smaller  $T_c$  and  $|\mu_c - m|$  occur with increasing parameter  $\lambda$ . Note that the BEC lines enter the (meta)stable regions of LGPT at low enough  $\mu$ .

The sensitivity of phase diagrams to the parameter  $\alpha$  is demonstrated in Fig. 9.

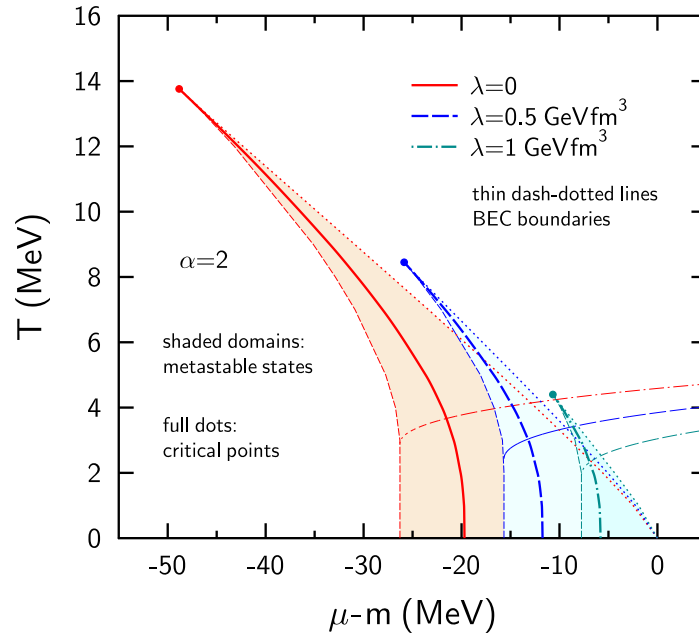


FIG. 8. Same as Fig. 7, but for  $\alpha = 2$ .

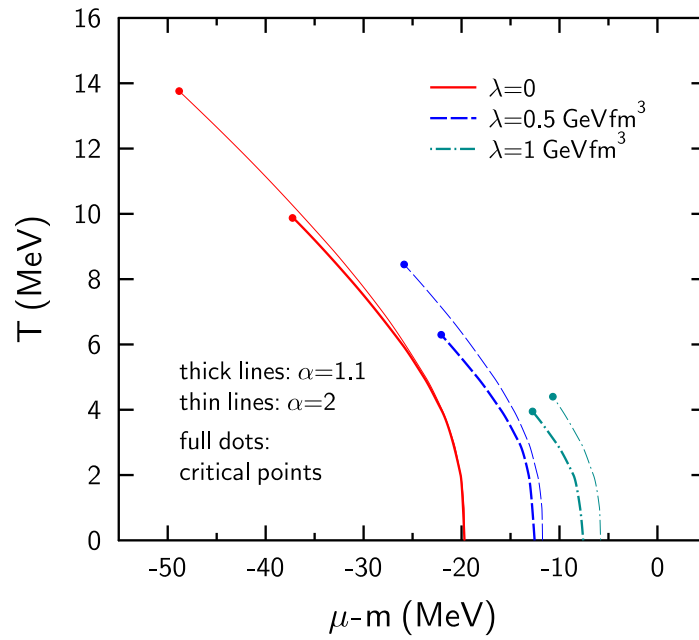


FIG. 9. Comparison of LGPT lines for  $\alpha = 1.1$  (thick) and  $\alpha = 2$  (thin) on the  $(\mu, T)$  plane. Dots represent positions of critical points.

## V. CONCLUSIONS

In the present paper we have investigated the sensitivity of the phase diagram of bosonic matter to the derivative interaction. We assume that the kinetic part of the Lagrangian contains the reduction factor  $F$  diminishing with the boson density. It is shown that this factor leads to an additional repulsion which significantly modifies the equation of state of bosonic matter as compared to the standard approach with  $F = 1$ . We have estimated maximal strength of the derivative interaction when both the liquid-gas phase transition and binding of bosonic matter disappear.

We think that the present approach will be useful for description of bosonic systems in laboratory experiments, as well as for predicting characteristics of boson stars and dark matter.

It would be interesting to extend current formalism by considering different parametrizations of the derivative interaction. One can use the present model for studying properties of finite bosonic systems (e.g. Q-balls). We believe that effects of the derivative interaction may be also important for fermionic systems.

## ACKNOWLEDGMENTS

Authors appreciate the support from the Frankfurt Institute for Advanced Studies.

- 
- [1] L. S. Kisslinger and F. Tabakin, *Phys. Rev. C* **9**, 188 (1974).
  - [2] T. H. R. Skyrme, *Phil. Mag.* **1**, 626 (1956).
  - [3] D. Vauterin and D. H. Brink, *Phys. Rev. C* **3**, 626 (1972).
  - [4] J. Zimanyi and S. Moszkowski, *Phys. Rev. C* **42**, 1416 (1990).
  - [5] Y. Chen, *Phys. Rev. C* **89**, 064306 (2014).
  - [6] A. Melchiorri, L. Mersini, J. Odman, and M. Trodden, *Phys. Rev. D* **68**, 043509 (2003).
  - [7] R. J. Scherer, *Phys. Rev. Lett.* **93**, 011301 (2004).
  - [8] A. K. Lloyd-Stubbs and J. McDonald, *Phys. Rev. D* **105**, 103502 (2022).
  - [9] L. M. Satarov, M. I. Gorenstein, A. Motornenko, V. Vovchenko, I. N. Mishustin, and H. Stoecker, *J. Phys. G* **44**, 125102 (2017).

- [10] L. M. Satarov, R. Poberezhnyuk, I. N. Mishustin, and H. Stoecker, Phys. Rev. C **103**, 024301 (2021).
- [11] L. M. Satarov, I. N. Mishustin, A. Motornenko, V. Vovchenko, M. I. Gorenstein, and H. Stoecker, Phys. Rev. C **99**, 024909 (2019).
- [12] L. M. Satarov, M. I. Gorenstein, I. N. Mishustin, and H. Stoecker, Phys. Rev. C **101**, 024913 (2020).
- [13] S. Elhatisari *et al.*, Phys. Rev. Lett. **106**, 132501 (2016).
- [14] L. M. Satarov, I. N. Mishustin, and H. Stoecker, Phys. Rev. C **106**, 014301 (2022).
- [15] W. von Oertzen, Lect. Notes Phys. **818**, 109 (2010).
- [16] G. Rosen, J. Math. Phys. **9**, 999 (1968).
- [17] R. Friedberg, T. D. Lee, and A. Sirlin, Phys. Rev. D **13**, 2739 (1976).
- [18] S. Coleman, Nucl. Phys. B **262**, 263 (1985); **269**, 744E (1986).
- [19] I. N. Mishustin, D. V. Anchishkin, L. M. Satarov, O. S. Stashko, and H. Stoecker, Phys. Rev. C **100**, 022201 (2019).
- [20] J. W. Clark and T.-P. Wang, Ann. Phys. (NY) **40**, 127 (1996).
- [21] L. Pitaevskii and S. Stringari, *Bose-Einstein Condensation*, (Clarendon Press, Oxford, 2000).
- [22] L. D. Landau and E. M. Lifshitz. *Statistical Physics* (Pergamon, Oxford, 1975).
- [23] E. M. Lifshitz and L. P. Pitaevskii. *Statistical Physics, Part2* (Pergamon, Oxford, 1980).
- [24] W. Greiner and J. Reinhardt. *Field Quantization*, (Springer, Berlin, 1996).